Tectonophysics 719-720 (2017) 148–161

Contents lists available at ScienceDirect

Tectonophysics

journal homepage: www.elsevier.com/locate/tecto

Onshore and offshore apatite fission-track dating from the southern Gulf of California: Insights into the time-space evolution of the rifting

Maria Laura Balestrieri [a,*], Luca Ferrari [b], Marco Bonini [a], Jose Duque-Trujillo [c], Mariano Cerca [b], Giovanna Moratti [a], Giacomo Corti [a]

[a] CNR, Consiglio Nazionale delle Ricerche, Istituto di Geoscienze e Georisorse, UOS Firenze, Via G. La Pira, 4, 50121 Firenze, Italy
[b] Centro de Geociencias, Universidad Nacional Autónoma de México, Campus Juriquilla, 76230, Querétaro, Qro., Mexico
[c] Universidad EAFIT, Medellin, Colombia

ARTICLE INFO

Article history:
Received 28 July 2016
Received in revised form 12 April 2017
Accepted 14 May 2017
Available online 17 May 2017

ABSTRACT

We present the results of a apatite fission-track (AFT) study on intrusive rocks in the southern Gulf of California, sampled along the eastern margin of Baja California Sur (western rift margin), as well as from islands and submerged rifted blocks within the Gulf of California, and from the conjugate Mexican margin (Nayarit state). For most of the samples U-Pb zircon and ^{40}Ar-^{39}Ar mineral ages were already available (Duque-Trujillo et al., 2015). Coupled with the new AFT data these ages provide a more complete information on cooling after emplacement. Our samples span a wide range of ages between 5.5 ± 1.1 and 73.7 ± 5.8 Ma, and show a general spatial distribution, with late Miocene AFT ages (about 6 Ma) aligned roughly NW-SE along a narrow offshore belt, parallel to Baja California Peninsula, separating older ages on both sides. This pattern suggests that in Late Miocene, deformation due to plate transtension focused at the eastern rheological boundary of the Baja California block. Some Early Miocene AFT ages onshore Baja California could be related to plutons emplaced at shallow depths and thermal resetting associated with the onset of volcanism at ~19 Ma in this part of the Peninsula. On the other hand, an early extensional event similar to that documented in the eastern Gulf cannot be ruled out in the westernmost Baja California.

1. Introduction and aims of the study

The Gulf of California corresponds to an active oblique-divergent plate boundary that separates the Baja California microplate from mainland Mexico, which is part of the North America Plate (Lonsdale, 1989; Dixon et al., 2000). At present, deformation is accommodated within the Gulf, where the relative plate motion between Baja California and North America occurs at a rate close to ~50 mm/yr (Plattner et al., 2007), and has generated an oblique rift characterized by long transform faults and short spreading centers (Lonsdale, 1989) (Figs. 1 and 2).

Three main models have been proposed to explain the time-space evolution, and the kinematics of the rifting. Two models agreed in that rifting started approximately in Late Miocene (~12–14 Ma) after the end of subduction of the Guadalupe and Magdalena microplates off the western margin of Baja California (Fig. 1) but propose a different kinematic history. In the first model continental extension in the Gulf of California occurred according to a two-phase kinematic evolution, in which a first phase of orthogonal rifting or "proto-Gulf" was followed by dextral-transtensional shearing within the Gulf beginning at ca. 6.5 Ma (Stock and Hodges, 1989; Lonsdale, 1991; Stock and Lee, 1994; Oskin et al., 2001). The model implies that between ~12.5 and 6.5 Ma motion between the Pacific and North America plates was partitioned into pure extension within the Gulf and pure dextral displacement west of Baja California Peninsula along the Tosco-Abreojos fault system (Fig. 1). The second model was initially proposed by Fletcher et al. (2007), who documented that motion along the Tosco-Abreojos fault system had been much less than previously believed, thus proposing that right lateral oblique rifting was ongoing within the Gulf since ~12.5 Ma. Since then other workers have also documented right lateral transtension in the northern part of the Gulf (e.g. Seiler et al., 2010; Bennet et al., 2013; Bennett and Oskin, 2014, and reference therein) but in general it has been agreed that the onset of rifting was at 14–12.5 Ma (see also Umhoefer, 2011 and references therein). A third group of studies have shown that extension in the Gulf region began much earlier than the end of subduction. Late Oligocene to middle Miocene extension has long been reported in the northeastern margin of the Gulf, in Sonora state (Gans, 1997; McDowell et al., 1997; Wong et al., 2010) and has been recently documented in the southeastern margin of the Gulf in Sinaloa and Nayarit (Ferrari et al., 2013) and within the southern Gulf (Duque-Trujillo et al., 2015) (Fig. 1). Ferrari et al. (2013) and Bryan et al. (2014) propose that the Gulf of California

* Corresponding author.
E-mail address: balestrieri@igg.cnr.it (M.L. Balestrieri).

http://dx.doi.org/10.1016/j.tecto.2017.05.012
0040-1951/

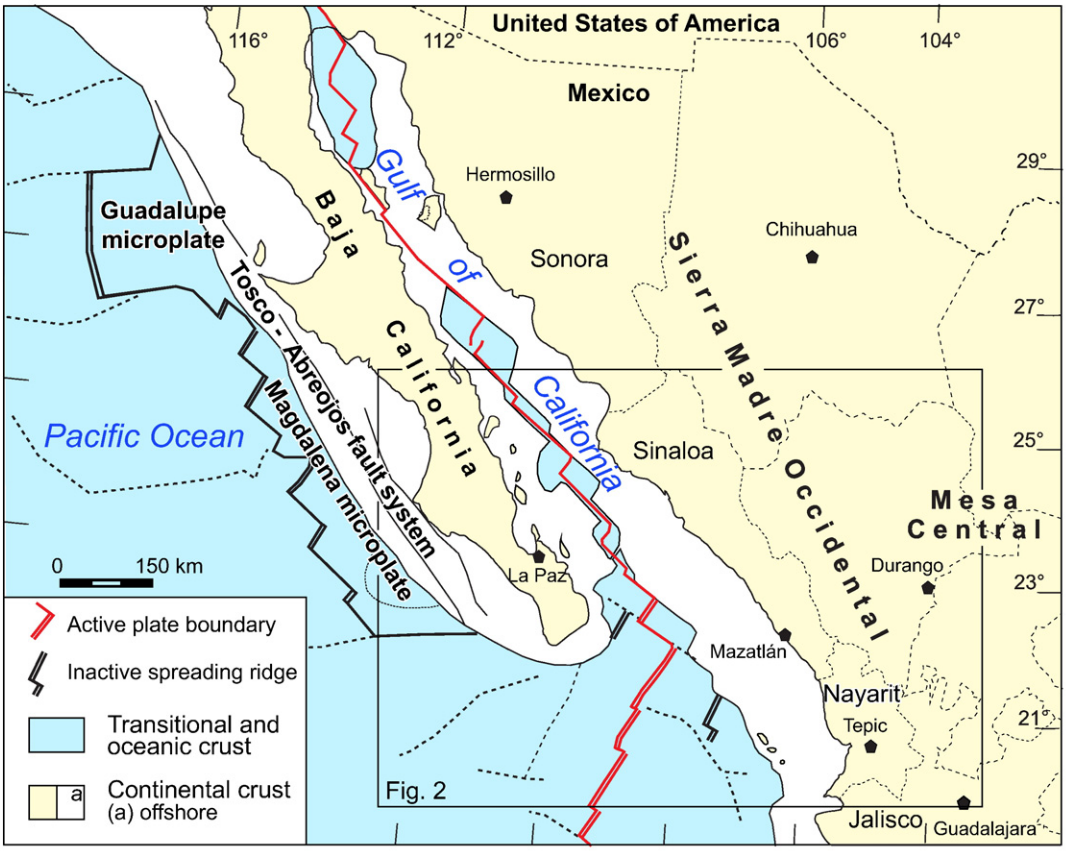

Fig. 1. Sketch map showing the main tectonic features of the Gulf of California.

evolved through a three-stage rifting process: (1) a wide-rift phase beginning in the late Oligocene in a region encompassing the Sierra Madre Occidental and the eastern part of Baja California (Fig. 1), (2) a focusing of the extensional deformation in the area of the present Gulf at ~18 Ma, and (3) development of transtensional deformation along the most thinned crust following the coupling between the Pacific plate and Baja California after the end of subduction (see also Ferrari et al., 2016, for a review).

To get some insights into this complex tectonic scenario, we have analyzed rock samples through apatite fission-track (AFT) method along a transect extending across the southern Gulf of California rift, from the eastern margin of Baja California Sur to onshore Mexico, in Nayarit, where intra-arc extensional structures of the western Trans-Mexican Volcanic Belt (Ferrari et al., 2012) intersects the mouth of the Gulf. Most of the samples were already dated via U-Pb and ^{40}Ar-^{39}Ar methods by Duque-Trujillo et al. (2015). Zircon U-Pb ages (closure temperature > 900 °C) are usually considered to reflect the age of intrusion (Cherniak and Watson, 2001) whereas ^{40}Ar-^{39}Ar closure temperatures are considered to reflect different cooling stages of intrusive rocks in the range 400–600 °C for hornblende, 270°–310 °C for biotite, and 150°–350 °C for K-feldspar (Alexandre, 2011; Reiners et al., 2005, and references therein). In case of shallow depth of emplacement, high-temperature thermochronometers (such as ^{40}Ar-^{39}Ar on hornblende and biotite) may yield ages overlapping with zircon U-Pb ages, simply representing crystallization age due to emplacement in country rocks cooler than the related system closure temperatures. AFT system, with a lower closure temperature of 110° ± 10 °C provides information on post-emplacement tectonic history of the intrusive bodies, when their cooling is related to the exhumation. Thus AFT data may shed light about timing and processes that brought the plutonic rocks to the surface provided that they intruded at depths where temperatures were higher than the total annealing temperature of the AFT system (ca. 120 °C, see section on the method). Our study contributes to understand the time-space deformation pattern of the Gulf of California and may help to determine the onset and migration of extensional faulting. Notably, this study reports - for the first time - the results of AFT dating from a number of samples submerged in deep-water Gulf of California, which were collected during the DANA (2004), ROCA (2008), and BEKL (2009) cruises (Duque-Trujillo et al., 2015). The AFT dating of such samples provides information for constraining the timing of deformation in such hardly accessible areas.

2. Geologic setting

The different magmatic and tectonic provinces that characterize the Western Mexico record the complex history of subduction and extension that have affected this continental margin of the North America Plate since the Cretaceous. A series of Cretaceous to Early Eocene batholiths represents the oldest episode of continental magmatism. Once forming a single NNW trending belt these intrusive bodies were later pulled apart by the extension and transtension that led the opening of the Gulf of California and are presently exposed along the Baja California peninsula (Peninsular Ranges Batholith) and on the Mexican mainland in Sonora and Sinaloa states (Ortega-Gutierrez et al., 2014). In southern Baja California they crop out in the Los Cabos block and several islands east of the Peninsula (Fig. 2). In the southern Gulf of California Cretaceous batholithic rocks have been dredged and sampled offshore on both margins, confirming the correlation between the granitoids exposed in the Los Cabos block with those in mainland Mexico. Collectively, prior to the rifting of Baja California, they formed a 150–200-km-wide igneous belt (Duque-Trujillo et al., 2015).

In the middle part of Baja California peninsula (north of La Paz), these batholiths are buried beneath an Eocene-to-Miocene cover made of sedimentary, volcanic and volcaniclastic deposits. The Early to Middle Miocene epiclastic and volcaniclastic sequences of the Comondú Group are the dominant rock units, which have been commonly referred to the construction/destruction phases of a volcanic arc (the Comondú arc) prior to the

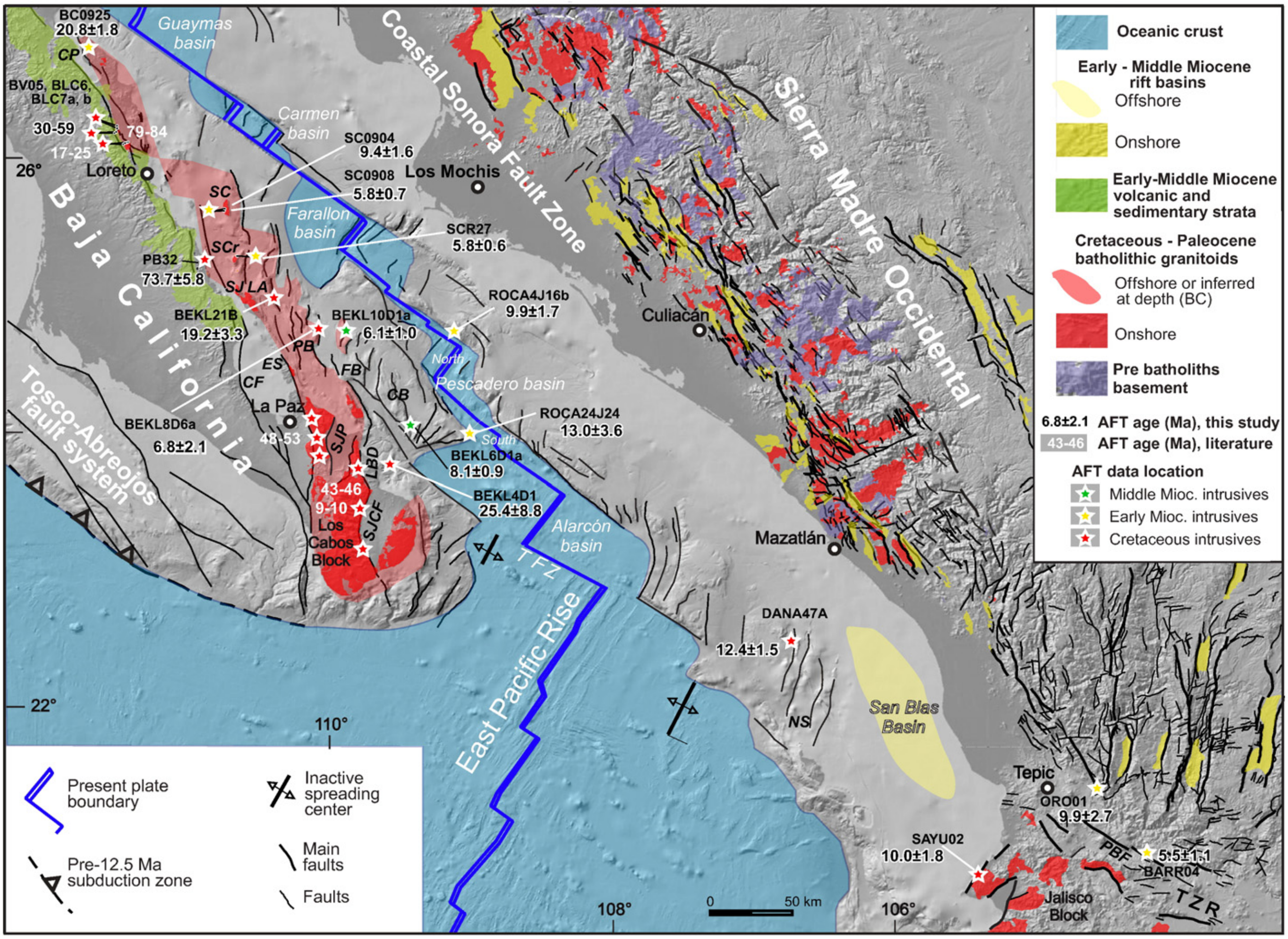

Fig. 2. Simplified geological-tectonic map of the southern Gulf of California (modified after Ferrari et al., 2016). Location of samples analyzed for AFT are shown together with age data from this study and reported in the literature (Los Cabos: Fletcher et al., 2000; Loreto: Mark et al., 2014). CP, Concepción Peninsula; SC, Isla Santa Catalina; SCr, Isla Santa Cruz; SJ, Isla San José; ES, Isla Espiritu Santo; PB, Partida Bank; CB, Cerralvo Bank; FB, Foca Bank; LA, Las Animas Bank; CF, Carrizal fault; SJP, San José de Los Planes fault; LCB, Los Barriles Detachment; PBF, Plan de Barrancas fault; SJCF, San José del Cabo fault; NS, Nayarit Scarp; TZR, Tepic-Zacoalco Rift.

rifting in the Gulf of California (e.g., Hausback, 1984; Fletcher et al., 2007; Umhoefer, 2011). In an alternative model, the Comondú Group is related to the deposition in a series of extensional basins developed since the Early Miocene in the area of the future Gulf of California, distributed between the Baja California peninsula and the western part of the Sierra Madre Occidental (Bryan et al., 2014; Ferrari et al., 2016).

Early and Middle Miocene plutons have intruded the Cretaceous–Paleocene batholiths of Baja California and its offshore continental rifted margin, as well as in mainland Mexico (Sinaloa, Nayarit and Jalisco states; Figs. 1 and 2) (Duque-Trujillo et al., 2015). In Nayarit and Jalisco a younger phase of transtension and extension formed the WNW-ESE trending Tepic–Zacoalco rift (Ferrari, 1995; Ferrari and Rosas-Elguera, 2000). The Tepic-Zacoalco rift branches off the southernmost part of the Gulf of California into the Trans-Mexican Volcanic Belt, the active continental volcanic arc that formed since the Miocene (Ferrari et al., 2012). Owing to the suitability of these rock types for thermochronology, sampling has targeted the Cretaceous batholiths as well as the Early and Middle Miocene plutons exposed in the southern Gulf of California and surroundings.

3. Apatite fission-track dating

3.1. AFT method

Fission-track thermochronology is considered an ideal technique for reconstructing the thermal history of rocks in the upper crustal levels. Fission tracks in minerals represent linear damage zones produced by the radioactive decay of ^{238}U (Wagner and Van de Haute, 1992). Over geological time, fission tracks are fully retained in apatite at temperature below 60 °C, while they are only partially retained between 60 °C and 120 °C (partial annealing zone, PAZ) with a mean closure temperature of 110°(±10)°C, assuming a cooling rate of 10 °C/Myr (Green and Duddy, 1989). Measurement of fission-track lengths gives information about the way the rocks cooled through the PAZ. The annealing behavior of fission tracks is sensitive to chemical composition. Diameter of etched spontaneous fission tracks measured parallel to apatite crystallographic c-axis (Dpar) is used as a proxy for track annealing kinetic properties (Barbarand et al., 2003; O'Sullivan and Parrish, 1995). A quantitative evaluation of thermal history can be obtained through the application of statistical modeling procedures that find temperature-time (T-t) paths compatible with the fission-track data (grain ages plus length distributions) (Gallagher, 1995; Ketcham, 2005; Ketcham et al., 2000). In many instances, because of low fission-track density, only few (or no) tracks can be measured in each sample. Because a statistically consistent distribution is well determined by ~100 measurements, modeling procedures cannot always be applied. Usually the grain-age distribution is subjected to a χ2 test to assess the homogeneity of AFT ages (Galbraith and Green, 1990; Galbraith and Laslett, 1993). A grain age distribution of an igneous rock sample failing the χ2 test (i.e. $P(\chi^2) < 5$) and showing high dispersion ($D > 20\%$) is indicative of a complex thermal history: it may indicate that (i) the rock

Table 1
Location and lithology of analyzed samples.

Sample	Location	Sample type	Lat (°N)	Long (°W)	Rock type
BV05	North of Loreto	Onshore, Baja California SE margin	26.2207	111.5547	Granodiorite
BLC6	North of Loreto	Onshore, Baja California SE margin	26.2407	111.5566	Granodiorite
BLC7a	North of Loreto	Onshore, Baja California SE margin	26.2202	111.5570	Granodiorite
BLC7b	North of Loreto	Onshore, Baja California SE margin	26.2212	111.5551	Granodiorite
PB32	Punta Botella	Onshore, Baja California SE margin	25.2911	110.9345	Quartz monzodiorite
BC0925	Bahia Concepcion	Onshore, Baja California SE margin	26.7827	111.7911	Monzogranite
SCR27	Santa Cruz Island	Island	25.3058	110.6997	Monzogranite
SC0904	Isla Santa Catalina	Island	25.6275	110.7934	Quartz monzonite
SC0908	Isla Santa Catalina	Island	25.6387	110.8004	Quartz monzodiorite
BEKL21B	Isla San Jose scarp	Dredge	24.9331	110.4116	Quartz monzodiorite
BEKL10D1a	Between Pescadero and Isla Espiritu Santo	Dredge	24.8081	109.9233	Monzogranite
BEKL8D6a	East of Partida bank	Dredge	24.7758	110.1308	Monzogranite
BEKL6D1a	S edge of Cerralvo Bank	Dredge	24.1140	109.45860	Monzogranite
BEKL4D1	Pescadero Canyon	Dredge	23.8280	109.6020	Monzogranite
ROCA4J16b	N Pescadero transform	Dive	24.7899	109.2008	Quartz monzodiorite
ROCA24J24	S Pescadero transform	Dive	24.0190	109.0390	Monzogranite
DANA47A	W Nayarit scarp	Dredge	22.5167	106.6992	Monzogranite
SAYU02	Sayulita, Nayarit	Onshore, Mexican conjugate margin, Sierra Madre Occidental	20.8685	105.4411	Monzogranite
ORO01	At the base of the Pochititán fault system, Sierra Madre Occidental margin, Nayarit	Onshore, Mexican conjugate margin, Sierra Madre Occidental	21.4640	104.5020	Monzogranite
BARR04	At the base of the Plan de Barrancas fault scarp, Tepic-Zacoalco rift	Onshore, Mexican conjugate margin, Sierra Madre Occidental	21.0204	104.1917	Tonalite

Notes: All sample locations are given using WGS84.

sample, after cooling at surface temperatures, has been partially reset by a successive thermal event or (ii) it resided for some time at partial annealing temperatures before ultimately cooling down during the final exhumation event that brought it to the surface. Radial plots (Galbraith, 1988), give a visual description of the age variability inside a sample because they show the single-grain ages. In this study, samples failing the χ^2-test or overdispersed are deconvolved in age peaks. The youngest peak with a concordant age (minimum age) represents the

Table 2
New fission-track ages from intrusive rocks from Southern Gulf of California.

Sample	$\rho_d \times 10^5$ (cm^{-2})	n_d	$\rho_s \times 10^5$ (cm^{-2})	n_s	$\rho_i \times 10^5$ (cm^{-2})	n_i	n_g	P(χ^2) %	D %	Central age ± 1σ (Ma)	U μg/g	Mean Dpar ± 1σ (μm)	n	Mean length μm ± 1σ (μm)	s.d.	n
BV05	8.35	3270	6.2	289	18.9	877	31	<1	34	49.0 ± 5.1	28.2	2.2 ± 0.4	96	–	–	–
BLC6	12.04	7004	3.5	148	18.3	770	25	29.9	11	40.7 ± 3.8	17.9	2.3 ± 0.3	59	–	–	–
BLC7a	12.06	7013	6.5	24	31.9	167	7	34.1	64	29.7 ± 10.8	34.11	2.1 ± 0.1	20	–	–	–
BLC7b	12.08	7019	9.3	268	33.2	958	24	34.8	0	58.6 ± 4.9	34.8	2.3 ± 0.3	30	–	–	–
PB32	8.33	3264	5.2	323	10.8	664	24	98.2	0	73.7 ± 5.8	15.4	2.0 ± 0.1	25	13.0 ± 0.2	1.57	43
BC0925	9.20	3603	7.6	190	61.2	1532	18	27.6	0	20.8 ± 1.8	77.0	4.6 ± 0.7	62	14.7 ± 0.2	1.12	29
SC0904	8.93	3499	1.2	39	20.1	679	22	52.8	0	9.4 ± 1.6	77.0	2.3 ± 0.5	33	–	–	–
SC0908	8.82	3455	1.1	87	30.6	2407	20	41.6	13	5.8 ± 0.7	68.5	2.3 ± 0.4	92	–	–	–
SCR27	8.36	3275	1.2	106	31.9	2771	27	53.6	101	5.8 ± 0.6	46.2	1.9 ± 0.3	81	–	–	–
BEKL21B	8.38	3282	0.5	44	3.7	354	31	63.9	11	19.2 ± 3.3	5.16	2.0 ± 0.2	32	–	–	–
BEKL10D1a	8.97	3514	0.6	41	15.6	1095	24	98.2	0	6.1 ± 1.0	18.9	1.9 ± 0.3	41	–	–	–
BEKL8D6a	8.34	3268	1.7	11	37.4	247	6	73.2	0	6.8 ± 2.1	44.2	2.1 ± 0.2	9	–	–	–
BEKL6D1a	9.16	3588	1.7	95	35.4	1955	20	95.8	0	8.1 ± 0.9	45.0	2.0 ± 0.3	75	–	–	–
BEKL4D1	8.32	3261	3.2	46	24.4	355	11	<1	89	25.4 ± 8.8	36.5	1.9 ± 0.2	22	–	–	–
ROCA4J16b	9.08	3558	0.6	37	10.3	617	24	76.7	0	9.9 ± 1.7	14.1	1.8 ± 0.2	39	–	–	–
ROCA24J24	8.78	3440	1.0	37	16.2	625	21	32.2	29	9.8 ± 1.9	23.3	1.7 ± 0.3	34	–	–	–
DANA47A	8.89	3485	1.0	83	12.7	1087	24	55.4	0	12.4 ± 1.5	19.2	1.7 ± 0.3	62	–	–	–
SAYU02	9.04	3544	1.1	52	17.7	840	21	68.3	14	10.2 ± 1.6	24.1	1.6 ± 0.3	72	–	–	–
ORO01	8.74	3426	0.8	15	12.4	243	14	87.2	0	9.9 ± 2.7	14.8	2.0 ± 0.3	18	–	–	–
BARR04	9.01	3529	0.4	29	11.7	864	25	75.2	0	5.5 ± 1.1	13.9	1.9 ± 0.2	86	–	–	–

Notes: Fission-track analysis was performed in the fission-track laboratory of the CNR, Institute of Geosciences and Earth Resources. Apatite grains were separated using standard heavy liquid and magnetic separation techniques. Mounts were ground, polished, and etched with 5 N HNO3 at 20 °C for 20 s to reveal the spontaneous tracks. The samples were then irradiated with thermal neutrons in the Lazy Susan facility of the Triga Mark II reactor of the LENA, University of Pavia (Italy). To measure the neutron fluence, standard glasses CN-5 were used as dosimeters. After irradiation, the low-U muscovite detectors were etched in 40% HF at 20 °C for 45 min to reveal the induced fission tracks. Ages determined by external detector method using a zeta value for dosimeter CN5 $\zeta = 360 \pm 11$ (referred to Fish Canyon Tuff and Durango apatite standards, Hurford, 1990). A Zeiss Axioskope microscope with dry objectives and 1250× magnification was used for apatite FT analysis.

ρ_d, ρ_i: standard and induced track densities measured on mica external detectors; ρ_s: spontaneous track densities on internal mineral surfaces, track densities are given in 10^5 tracks cm^{-2}; n_d, n_i and n_s: number of tracks on external detectors and on mineral surfaces; n_g: number of counted mineral grains; P(χ^2): (χ^2) probability (Galbraith, 1981); Central age calculated using TRACKKEY program (Dunkl, 2002); Dpar: mean etch pit diameter parallel to the c-axis and number (n) of total measured Dpar for sample; Lm: mean length of confined tracks length distribution ± standard error, s.d.: standard deviation, n: total measured lengths, only TINTs (tracks reached by the etching because they intercept a surface track, Bhandari et al., 1971) were measured, as recommended by Ketcham (2005). Single-grain data available at www.pangaea.de, PDI-14761.

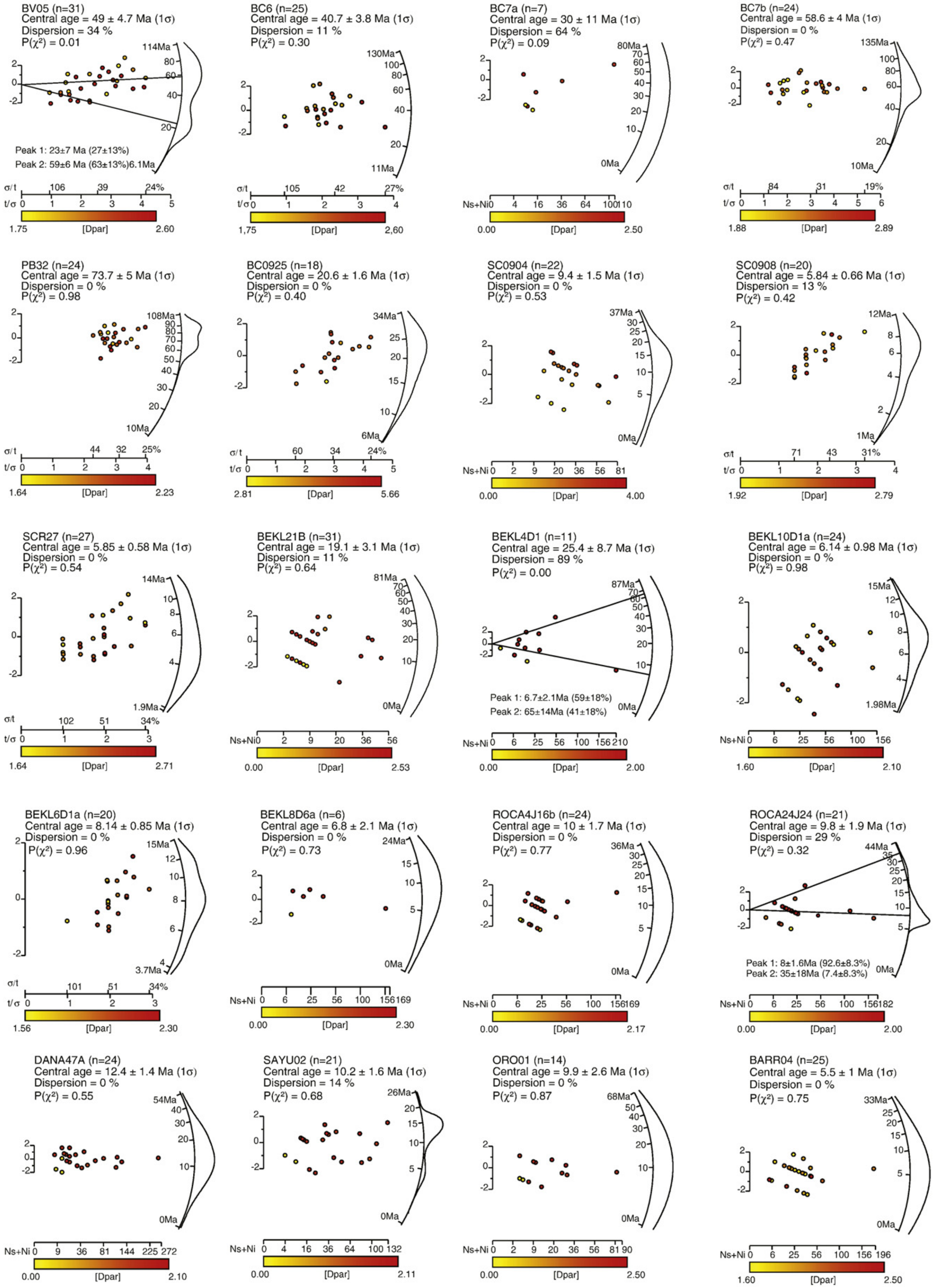

Fig. 3. Radial plots with abanico curves of apatite fission-track data drawn with Radial Plotter program (Vermeesch, 2009). Each dot represents a crystal; the age can be read on the intersection between a line linking the origin with a dot and the arc; the precision in age is reported on the x axis. Bars on the y axis indicate the standard error of each measurement.

population formed by the less retentive grains that record the time of final cooling. The minimum age corresponds to the time when the sample cooled to a temperature outside the partial annealing zone (Brandon et al., 1998) (apatite PAZ, top ca. 60 °C). Therefore, minimum age allows recognition of the time of exhumation also from partially reset or samples residing for a time span inside the PAZ before ultimately cooling to surface temperatures.

3.2. Results of the AFT analysis

Apatites separated from twenty intrusive rock samples have been dated by the fission-track method to extend their cooling/exhumation path up to shallower levels in the crust. Not all the samples were of good quality so that in some cases few apatite grains could be counted. The samples were collected both onshore and offshore on the two rifted margins of the southern Gulf of California (Fig. 2). Information about location and petrography of the analyzed samples are reported in Table 1. Subaerial sampling sites include: (1) intrusive rocks exposed north of Loreto, at Punta Botella, Bahía Concepción, and on islands off the eastern coast of Baja California, and (2) the western Mexico margin in the state of Nayarit (Figs.1 and 2). Submarine samples mostly come from the rifted continental crust offshore Baja California, including Cretaceous batholiths as well as the Early to Middle Miocene plutons (Fig. 2). Other samples have been collected along scarps of the sheared margins of the Northern and Southern Pescadero basins, and at the Nayarit scarps (Fig. 2). More information of the geologic context of these samples is provided in Duque-Trujillo et al. (2015).

Table 2 reports the details of the fission-track data determination. The young fission-track age of most samples and the intermediate-to-low U concentration prevented the measure of track lengths in most of the analyzed samples. In Fig. 3, radial plots of all the analyzed samples are reported. In Table 3 the U-Pb and ^{40}Ar-^{39}Ar ages of Duque-Trujillo et al. (2015) are reported together with the AFT ages obtained in this study to make the comparison easier. These ages are also shown in Figs. 4, 5 and 6. In the following we briefly describe the AFT results for each sample according to their geographic location.

3.2.1. Onshore, western rifted margin in Baja California

Samples from intrusive rocks exposed in the eastern part of Baja California Peninsula show the oldest AFT ages. Four samples (BV05, BLC6, BLC7a, BLC7b) from granodiorite batholitic rocks exposed 25 km NNW of Loreto yielded AFT ages spanning between 58.6 ± 4.9 Ma and 29.7 ± 10.8 Ma. Sample BV05 fails the χ^2-test and samples BLC6 and BLC7a are overdispersed, even if they pass the χ^2-test (Table 2, Fig. 3). Sample BV05 where 31 grains were dated, was deconvolved using the radialplotter software of Vermeesch (2009), and it shows two peaks, one of 58.9 ± 5.7 Ma and one of 22.8 ± 6.6 Ma (Fig. 3).

These samples are the only ones not dated in Duque-Trujillo et al. (2015). However, they were collected in the same bodies dated at ca. 91 and 103 Ma by zircon U-Pb method by Mark et al. (2014). All the U-Pb and ^{40}Ar-^{39}Ar ages mentioned in the remainder of this section are from Duque-Trujillo et al. (2015), which is not further cited. Sample PB32 is a quartz-monzodiorite from Punta Botella, located on the coast 90 km south of Loreto, with a zircon U-Pb age of 100.4 ± 1.3 Ma. This sample yielded an AFT age of 73.7 ± 5.8 Ma with a mean track length of 13.0 ± 0.2 μm on a length distribution composed of only 43 determinations. BC0925 is an Early Miocene monzogranite (U-Pb zircon age of 19.9 ± 0.6 Ma) that show a very close ^{40}Ar-^{39}Ar biotite age of 19.3 ± 0.3 Ma, from the footwall of a west-dipping normal fault system that bounds the western side of Concepción Peninsula, about 85 km north of Loreto (Fig. 2). The determined AFT age is 20.8 ± 1.8 Ma with a long mean length of 14.7 ± 0.2 μm but calculated from an even a more restricted distribution of 29 determinations only.

3.2.2. Islands off the eastern coast of Baja California

Samples from two islands offshore Baja California yielded young AFT ages. SC0904 and SC0908 are Early Miocene quartz-monzonite that crops out in the western part of the Santa Catalina Island (Fig. 1) and show a similar cooling history (Table 3). They have almost identical ^{40}Ar-^{39}Ar ages on hornblende and biotite at ~18–19 Ma likely related to the plutonic bodies emplacement but a much younger AFT age of 9.4 ± 1.6 Ma for SC0904 and 5.8 ± 0.7 Ma for SC0908. Sample SCR27, from a Cretaceous monzogranite (zircon U-Pb 98.5 ± 1.5 Ma) exposed at Santa Cruz Island, also yielded an AFT age of 5.8 ± 0.6 Ma.

3.2.3. Offshore samples from the southern Gulf of California

Samples from the western rifted margin between Baja California and the Farallón and Pescadero oceanic basins show variable AFT ages. Two Late Cretaceous intrusive rocks sampled within 20 km from the Baja California coast show AFT ages similar to those in the eastern part of the Peninsula. BEKL21B, a quartz-monzodiorite dredged on the normal fault scarp bounding the San Jose island to the east, shows an AFT cooling age of 19.2 ± 3.3 Ma. For the monzogranite BEKL4D1, dredged 11 km offshore on the rifted margin of the Los Cabos Block (Fig. 2), we obtained an AFT age of 25.4 ± 8.8 Ma but it fails the χ^2-test. Actually, the deconvolution of the grain age distribution gives two peaks, P1 at 6.7 ± 2.1 Ma and P2 at 65 ± 14 Ma (Fig. 3).

Three samples from a highly extended belt, comprised between San Jose, Espiritu Santu, Cerralvo islands to the east and the Pescadero basin to the west, yielded Late Miocene AFT ages. BEKL10D1a is a monzogranite dredged from a bank between the northern Pescadero basin and the Isla Espiritu Santo. This sample has a U-Pb zircon age of 13.4 ± 0.1 Ma, a ^{40}Ar-^{39}Ar biotite age of 12.6 ± 0.1 Ma, and yielded an AFT age of 6.1 ± 1.0 Ma. BEKL6D1a is also a middle Miocene monzogranite that was dredged on the eastern margin of the Cerralvo bank (Fig. 2) and has a U-Pb zircon age of 15.4 ± 0.1 Ma, a ^{40}Ar-^{39}Ar age of 13.7 ± 0.3 Ma on hornblende, and 13.4 ± 0.2 Ma on biotite. The AFT age of this sample is 8.1 ± 0.9 Ma. The monzogranite BEKL8D6a was dredged 20 km to the west of BEKL10D1a, on the eastern edge of the Partida Bank. For this sample, which has Late Cretaceous U-Pb and ^{40}Ar-^{39}Ar ages (Table 3), we obtained an AFT age of 6.8 ± 2.1 Ma.

By contrast, two samples from the sheared margins of the northern Pescadero basin yielded AFT ages older than the belt to the west. ROCA4J16b is a quartz-monzodiorite sampled on the scarp of the northern Pescadero transform and bounding the basin to the NE. The sample has a U-Pb zircon age of 25.1 ± 0.7 Ma and a ^{40}Ar-^{39}Ar K-feldspar age of 11.1 ± 0.8 Ma, very close to the newly determined AFT age of 9.9 ± 1.7 Ma.

ROCA24J24 is a monzogranite sampled on the scarp of a strike-slip fault associated with the southern Pescadero transform, near its junction with the Alarcón basin. This sample has a U-Pb age of 20.1 ± 0.2 Ma on zircon and a ^{40}Ar-^{39}Ar biotite age of 13.8 ± 0.1 Ma. The newly determined AFT age is 9.8 ± 1.9 Ma. The sample grain age distribution passes the χ^2-test but it is slightly overdispersed (29%). The deconvolution of the grain age distribution gives two peaks, P1 at 8 ± 1.6 Ma and P2 at 35 ± 18 Ma (Fig. 3). Finally, sample DANA47 was dredged on the western Nayarit scarp, on the eastern side of the Alarcón basin. This sample is a Late Cretaceous monzogranite with a U-Pb zircon age of 92.9 ± 0.9 Ma and a ^{40}Ar-^{39}Ar biotite age of 19.2 ± 0.1 Ma. The AFT age is 12.4 ± 1.5 Ma.

3.2.4. Onshore, eastern rifted margin on Mexico mainland

Two samples from the rifted margin in Nayarit present AFT ages similar to those surrounding the Pescadero and Alarcón basins. SAYU02 comes from a Late Cretaceous monzogranite sampled along the NNE striking southeastern rifted margin of the Jalisco Block (Fig. 2). Zircon U-Pb age is 75.2 ± 0.5 Ma and ^{40}Ar-^{39}Ar biotite age is 43.9 ± 0.2 Ma. The newly determined AFT age is much younger being 10.2 ± 1.6 Ma.

Table 3
Available chronology data on studied samples. Samples are grouped according their zircon U-Pb age.

Sample	U-Pb Zr age	Ar-Ar Hbl age	Ar-Ar Bt age	Ar-Ar K-fsp age	AFT age
Cretaceous					
PB32	100.4 ± 1.3				73.7 ± 5.8
SCR27	98.2 ± 1.5				5.8 ± 0.6
BEKL21B	95.4 ± 2.2				19.2 ± 3.3
BEKL8D6a	96.7 ± 1.1	94.5 ± 1.4 tc	96.8 ± 0.3		6.8 ± 2.1
BEKL4D1	82.4 ± 0.7		75.6 ± 2.4		25.4 ± 8.8
DANA47A	92.9 ± 0.9	–	19.6 ± 0.1		12.4 ± 1.5
SAYU02	75.2 ± 0.5	–	43.9 ± 0.2		10.2 ± 1.6
Early Miocene					
BC0925	19.9 ± 0.6		19.3 ± 0.3 tp		20.8 ± 1.8
SC0904	–	19.0 ± 0.3	19.5 ± 0.2 tc		9.4 ± 1.6
SC0908	22.2 ± 0.4	18.9 ± 0.5	18.4 ± 0.1		5.8 ± 0.7
ROCA4J16B	25.1 ± 0.7			11.1 ± 0.9	9.9 ± 1.7
ROCA24J24	20.1 ± 0.2		13.8 ± 0.1		13.0 ± 3.6
ORO01	21.3 ± 0.5	19.1 ± 0.2		17.6 ± 0.1	9.9 ± 2.7
BARR04	22.7 ± 0.4	19.8 ± 0.5	19.6 ± 0.1		5.5 ± 1.1
Middle Miocene					
BEKL10D1a	13.7 ± 0.2		12.6 ± 0.1		6.1 ± 1.0
BEKL6D1a	15.4 ± 0.1	13.7 ± 0.3	13.4 ± 0.2		8.1 ± 0.9

Notes: tc and tp are isochron and plateau age, respectively.

The age grain distribution is not overdispersed (D = 14%) thus we do not deconvolve it but the abanico curve suggests two age populations (Fig. 3). ORO01 is a monzogranite sampled along a NNW striking normal fault system that bound the Sierra Madre Occidental in northern Nayarit. It has a U-Pb zircon age of 21.3 ± 0.5 Ma and ^{40}Ar-^{39}Ar ages of 19.1 ± 0.2 Ma on hornblende and 17.6 ± 0.1 Ma on feldspar. Here the AFT age is 9.9 ± 2.7 Ma.

On the other hand, BARR04 sampled within the Tepic-Zacoalco rift in eastern Nayarit, yielded a younger age. This is a tonalite exposed in the footwall of the Plan de Barrancas normal fault system, which has a U-Pb zircon age of 22.7 ± 0.4 Ma, and a ^{40}Ar-^{39}Ar age of 19.8 ± 0.5 Ma on hornblende and 19.6 ± 0.1 Ma on biotite. It yielded an AFT age of 5.5 ± 1.1 Ma.

4. Data interpretation

The new AFT data, coupled with previous U-Pb and Ar-Ar geochronology can be interpreted in term of four different cooling domains, which correspond to tectonic domains within the southern Gulf of California. From west to east they are: 1) the western rifted margin comprising the eastern part of Baja California and its nearby offshore extension; 2) a belt comprising some of the islands offshore Baja California and a submerged stretched crust west of Pescadero and Farallón oceanic basins; 3) the sheared margins of the Pescadero basin and the eastern rifted margin west of the Jalisco Block and the Sierra Madre Occidental; 4) the Tepic-Zacoalco rift. In the following we discuss each of these domains.

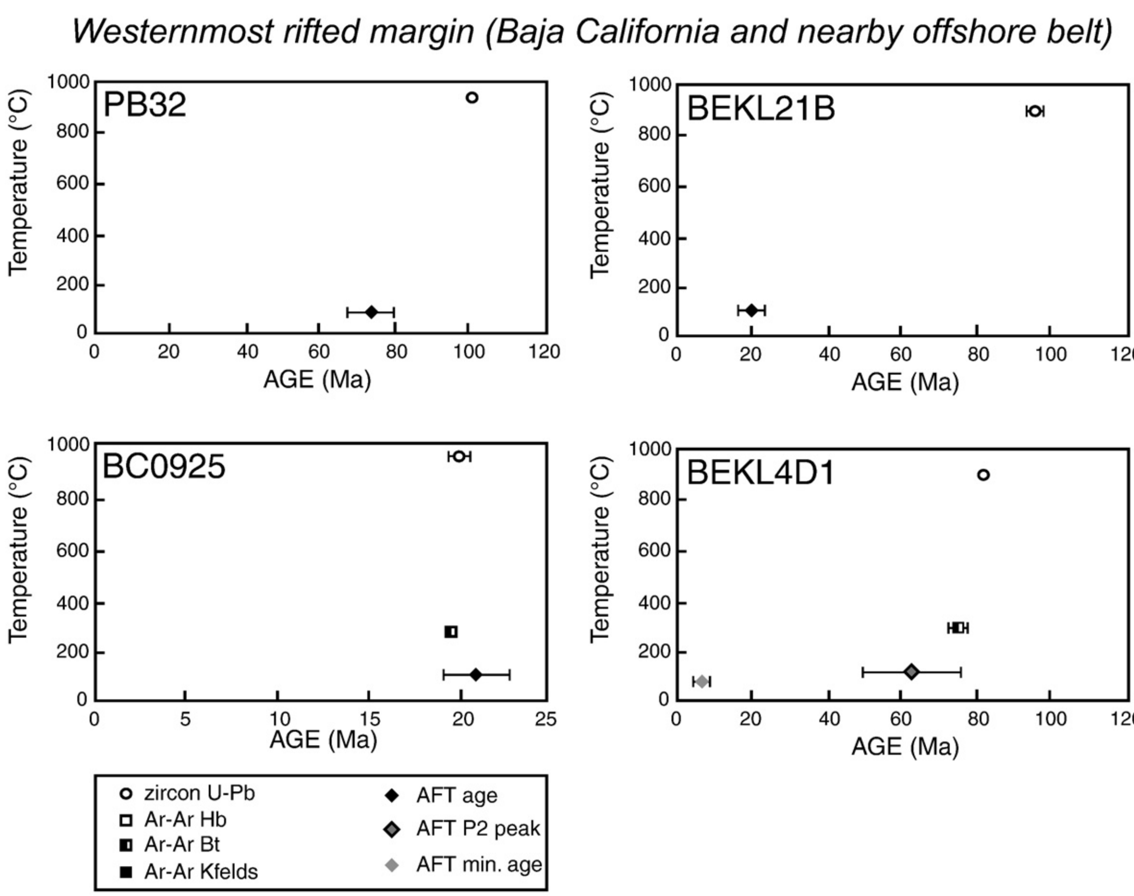

Fig. 4. Plots of the available age data with respect to the closure temperatures of the respective geochronological system to reconstruct possible cooling paths. Samples from the westermost rifted margin.

4.1. Westernmost rifted margin (Baja California and nearby offshore belt)

This belt comprises samples PB32, BV05, BLC6, BLC7a, BLC7b, BC0925, PB32, BEKL21B and BEKL4, which show Early Miocene or older AFT ages. The four samples (BV05, BLC6, BLC7a, and BLC7b), coming from Cretaceous intrusive bodies north of Loreto, show a range of AFT age spanning between 59 and 30 Ma. The samples lie on the footwall of ENE-dipping normal faults, east of the Main Gulf Escarpment of Baja California. These samples come from the same isolated outcrops of granodiorites studied by Mark et al. (2014), who consider them laying on a piedmont denudated from the westward retreat of the escarpment from a rift-bounding fault. In particular, the fault development has been constrained to ca. 8–6 Ma on the basis of apatite (U-Th)/He (AHe) dating (4.8–7.6 Ma; Mark et al., 2014). Mark et al. (2014) reported two groups of AFT ages of 17–25 Ma and 79–84 Ma for their southern and northern transects, respectively (Fig. 2). Our sample PB32 showing the oldest AFT age has been collected along the coast at Punta Botella on the footwall of a W-dipping normal fault parallel to the coast (Duque-Trujillo et al., 2015) (Fig. 2). It shows a 73.7 ± 5.8 Ma AFT age comparable to Mark's et al. (2014) ages from the northern transect. These authors relate the Early Miocene AFT ages found along their southern transect to a localized heating event at ca. 22–18 Ma. They considered that it was a local event because of the older ages shown by the samples from the nearby northern transect. Our other onshore samples from the Cretaceous batholiths, show a wider range of AFT ages likely indicating that they were affected by a thermal event that only partially reduced their ages. Thus, we propose that our samples north of Loreto, as well as those of Mark et al. (2014), may have experienced a heating event in Early Miocene times, after their emplacement and cooling in the Late Cretaceous. This heating event affected the samples at different degree, with partial or total resetting of the AFT system. For sample BV05, that fails the χ^2-test, the P1 peak age of 22.8 ± 6.6 Ma may represent the cooling after the heating event of Early Miocene that would be consistent with the with Mark's et al. (2014) southern transect results. Similarly, the Early Miocene AFT ages of the Cretaceous intrusive offshore sample BEKL21B (19.2 ± 3.3 Ma), which passed the χ^2-test and it is not overdispersed, may be interpreted as a cooling age after a total reset caused by an Early Miocene thermal event. Given that these samples and that north of Loreto are about 200 km apart, this Early Miocene heating event had likely a regional extent. Its timing coincides with the onset of volcanism along the eastern part of southern Baja California (Ferrari et al., 2016) with several dacitic domes emplaced in a NNW alignment along the Loreto escarpment (Hausback, 1984; Umhoefer, 2011; Godinez et al., 2010). Moreover, the recent study of Duque-Trujillo et al. (2015) revealed that the Early-Middle Miocene plutons are not sparse occurrences but constitute an extensive suite emplaced

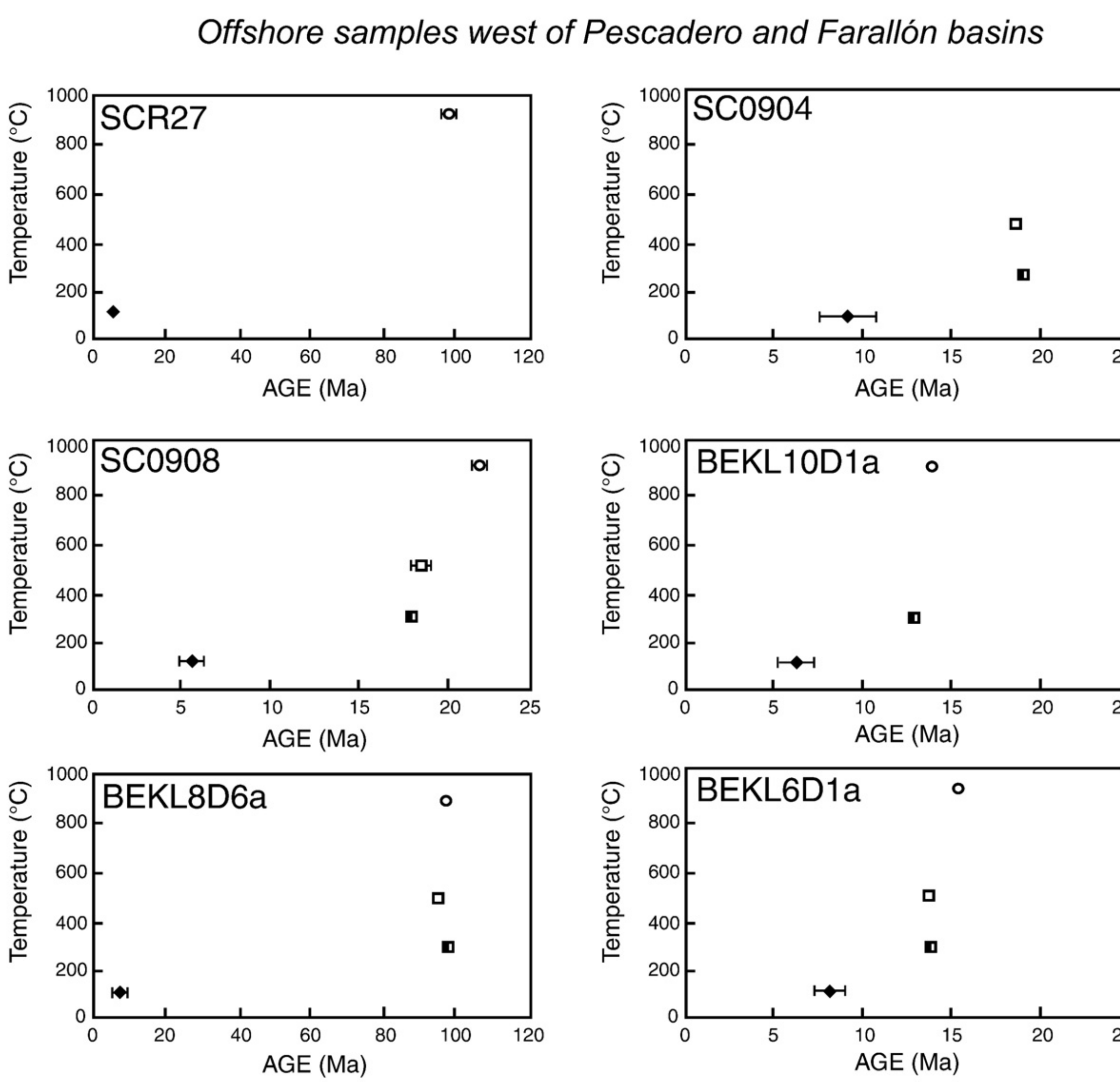

Fig. 5. Plots of the available age data with respect to the closure temperatures of the respective geochronological system to reconstruct possible cooling paths. Offshore samples west of Pescadero and Farallón basins. Symbols are as those of Fig. 4.

at shallow depths within the belt of the Peninsular Ranges batholith. In particular, Duque-Trujillo et al. (2015) recognized a distinctive group of high silica granites emplaced in Early Miocene and defining an elongated WNW-ESE-trending belt crossing the entire southern Gulf of California, from southern Baja California to Nayarit and Sinaloa conjugate margins in mainland Mexico. On this basis, our new samples may indicate a heating event with a regional extent that could be related to the onset of local volcanism and emplacement of the early Miocene group of plutons. In turn, the latter may be interpret as the intrusives correspondent of the volcanic rocks or as expression of a regional extensional regime.

The Early Miocene intrusive collected near the west dipping normal fault zone bounding the east side of Bahía Concepción (BC0925), yield overlapping U-Pb zircon, ^{40}Ar-^{39}Ar biotite and AFT ages of ca. 20 Ma within 1σ error. This setting indicates that the sample cooled through the AFT closure temperature (ca. 110 °C) immediately after the emplacement (Fig. 4; Table 3). Twenty-nine track lengths show a long mean length of 14.7 ± 0.2 μm, confirming a very rapid cooling. When interpreting this sample's age, two possibilities arise: i) the intrusive body was emplaced at very shallow levels and the three overlapping ages, represents essentially crystallization ages, ii) the intrusive body was lifted to the surface along a fault plane quickly after the emplacement. The sample lies very close to a major system of normal faults (Concepción Bay Fault Zone of McFall, 1968) and comes from a small body 1.5 km west of the main body of the Cerro Blanco tonalite mapped by McFall (1968), for which a 20 Ma K-Ar age is available. At our sampling site the body intrudes an undated ignimbrite, which should correspond to the lower member of the Comondú Fm. The sample shows a fine grained and porphyritic texture. Given the sample texture and geological context, it represents a shallow intrusion, likely emplaced even above the lower limit of the PAZ. However, it is also in close proximity to a major west dipping extensional fault zone that bounds Peninsula Concepción to the west (Fig. 7). It is important to note that this fault zone (Concepción Bay Fault Zone of Mc Fall, 1968) has an opposite vergence with respect to that of the late Miocene faults bounding the modern Gulf of California. According to McFall (1968), the Concepción Bay Fault Zone started to form in the late Oligocene (~28 Ma) and continued for the subsequent 15 Ma. In conclusion, we consider that although our data can be easily explained by a rapid cooling below the apatite PAZ due to a very shallow depth of emplacement of the sampled intrusive body, the possibility that an extensional fault zone was also active at this time and responsible for bringing

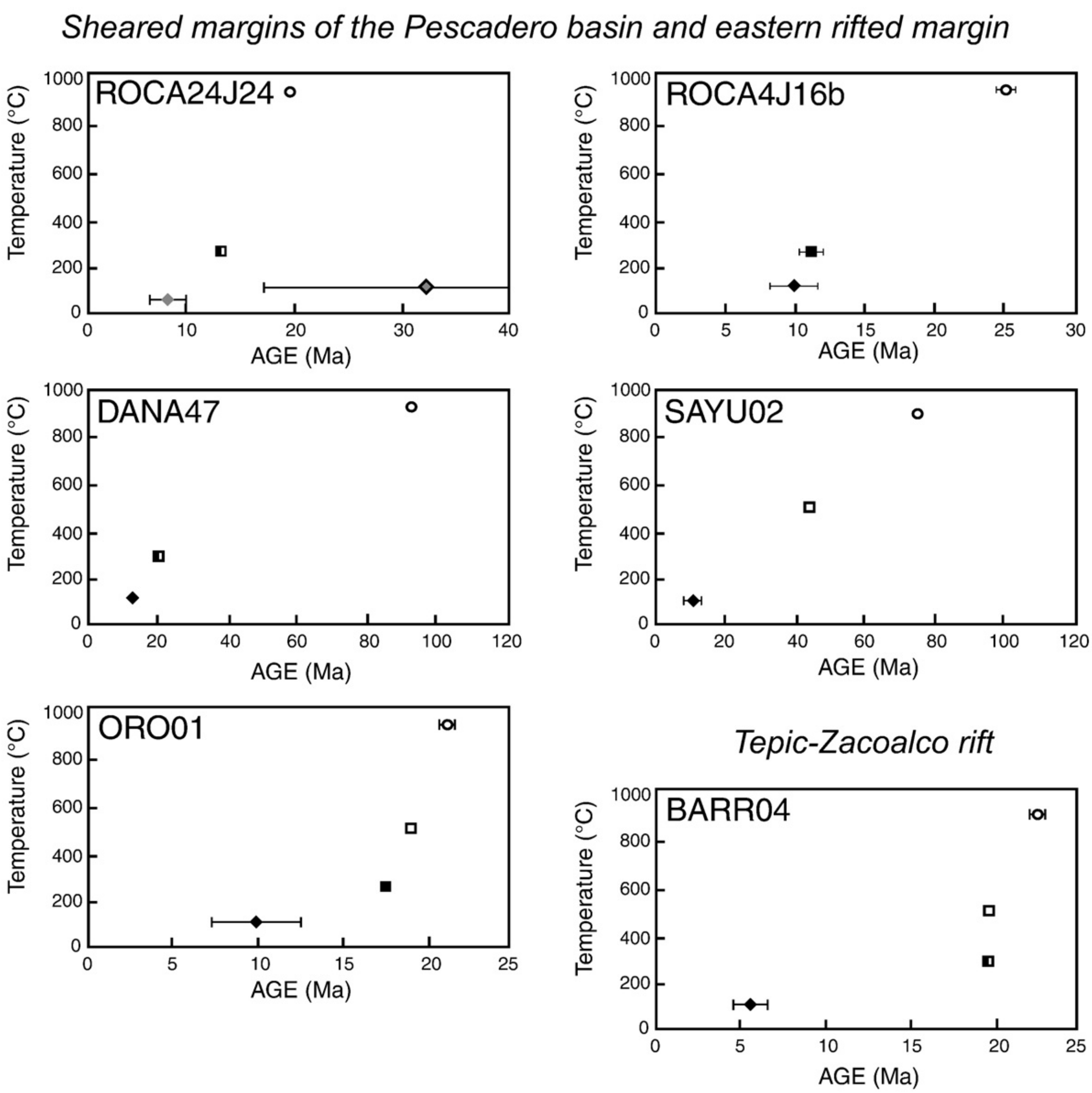

Fig. 6. Plots of the available age data with respect to the closure temperatures of the respective geochronological system to reconstruct possible cooling paths. Samples from the sheared margin of the Pescadero basin and eastern rift margin and from Tepic-Zacoalco rift. Symbols are as those of Fig. 4.

close or even at the surface an intermediate to shallow intrusion, cannot be ruled out.

A possible support to the occurrence of an early extension in this part of the Gulf may be found in the recent works at the southern tip of the Baja California peninsula, where the Cretaceous batholith of the Los Cabos block is rifted by the roughly N-S-trending, E-dipping San José del Cabo normal fault system (Fig. 2). Fletcher et al. (2000) reported zircon and apatite fission-track ages for three samples from the footwall of the Los Cabos fault indicating rapid exhumation at 12–10 Ma. However, their samples are from the base of a major fault scarp with over 1.5 km of displacement and likely they are not recording the timing of fault activation but rather its end. The onset of activity in the northern segment of the Los Cabos fault system has been recently dated at ~18.05 Ma by dating the hydrothermal activity associated to the Los Barriles detachment (Bot et al., 2016).

The other Cretaceous intrusive sample BEKL4D1, dredged offshore to the south respect to BEKL21B, which shows a late Oligocene to Early Miocene AFT age (25.4 ± 8.8 Ma), fails the χ^2-test and show a young peak at 6.7 ± 2.1 Ma. This sample may record a partial reset or a long permanence in the apatite PAZ before ultimately cooling through the top of the apatite PAZ in late Miocene times. This result better ascribes sample BEKL4D1 to the following domain.

4.2. Offshore samples west of Pescadero and Farallón basins

AFT ages determined on other 6 offshore samples (including islands) range between 9.9 ± 1.3 and 5.8 ± 0.6 Ma (SCR27, SC0904, SC0908, BEKL10D1a, BEKL8D6a, and BEKL6D1a). These samples come from a NW trending belt west of the Pescadero and Farallón basins and limited by NW-striking right lateral shear zones along the prolongation of the Alarcón and Pescadero transform faults (Fig. 2). The belt, which includes the Cerralvo, Foca, Partida, and Las Animas banks as well as the Santa Catalina and Santa Cruz islands (Fig. 2), is dissected by ~N-S striking faults with en echelon array, which suggest a right lateral transtensional deformation. Although fission-track length could not be measured in these samples, we tentatively interpret these ages as cooling ages, given that they pass the χ^2-test and they are not overdispersed. Estimates of emplacement depth are available only for two middle Miocene intrusives BEKL10D1a and BEKL6D1a, between 3 and 6 km and 3 and 7 km, respectively (Duque-Trujillo et al., 2015). Considering plausible values for the geothermal gradient (25°-30 °C/km), such depths are sufficient to have fully reset samples prior to their unroofing by faulting in a transtensional environment. Actually, all these samples have been collected on the footwall of major faults (see Fig. 2), and thus the AFT data are expected to reveal the age of rift escarpment exhumation produced by the fault activity. Most of these samples show a similar history, with rapid cooling up to the ^{40}Ar-^{39}Ar hornblende or biotite closure temperature (and overlapping hornblende and biotite ages when both are available), followed by a Late Miocene final cooling to the AFT temperature (Table 3, Fig. 5). Three Cretaceous intrusive rocks coming from Santa Cruz Island (SCR27) and Santa Catalina Island (SC0904 and SC0908) have AFT ages indicating a Late Miocene cooling below 110 °C between 9.5 and 6 Ma (Figs. 2 and 3). A sample of the Cretaceous batholith collected East of the Partida bank (BEKL8D6a) has zircon U-Pb, hornblende and biotite ^{40}Ar-^{39}Ar ages that overlap within the error, pointing to a very rapid cooling up to 350°-270 °C in the Late Cretaceous, which is followed by AFT age indicating a last exhumation in the Late Miocene at ~6.8 Ma (Fig. 5). An intrusive rock belonging to the Middle Miocene group (BEKL10D1a), dredged from a bank between the northern Pescadero basin and the Espiritu Santo Island, points to a rapid cooling below 310°-270 °C in the Middle Miocene (U-Pb zircon age of ~14 Ma and biotite age of ~12.6 Ma) followed by a final exhumation at ~6 Ma (Fig. 5). Sample BEKL6D1a, collected at the Cerralvo bank, was intruded at ~15 Ma and cooled below the biotite closure temperature at ~13 Ma, but has a final exhumation in Late Miocene as witnessed by the AFT age of ~8 Ma (Fig. 5). Our new AFT age indicate that this NNW-trending belt, bounded by the prolongation of the southern Pescadero and Alarcón transform faults, has been activated toward the end of the Late Miocene, probably in a right lateral transtensional deformation regime.

4.3. Sheared margins of the Pescadero basin and eastern rifted margin

Two samples with Early Miocene intrusion ages on both sides of the Pescadero basin show a similar history. The intrusive rock collected on the fault scarp bounding the southern Pescadero basin at its junction with the Alarcón basin (ROCA24J24) was emplaced at ca. 20 Ma and cooled through the 310°-270 °C isotherms at 13.7 Ma. The AFT

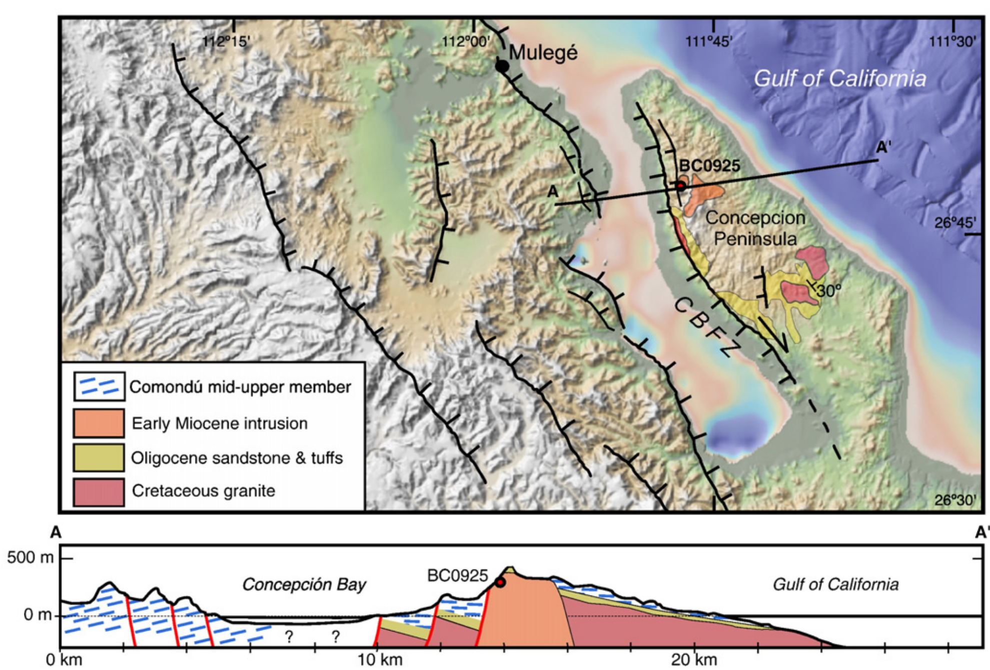

Fig. 7. Geologic sketch map of the Bahía Concepción area showing the location of sample BC0925. Geology based on McFall (1968) and our reconnaissance mapping. CBFZ = Concepción Bay Fault zone.

minimum age of 8.0 ± 1.6 Ma may indicates a last cooling to surface temperatures at the beginning of late Miocene (Figs. 3, 6). Sample ROCA4J16b, collected from the scarp bounding to the NE the northern Pescadero basin, was emplaced at ca. 25 Ma but shows ^{40}Ar-^{39}Ar K-feldspar and AFT ages overlapping within the error at about 10–11 Ma.

Three other samples from faults of the eastern rifted margin of the Gulf yielded very similar AFT ages at ~10–12 Ma but older ^{40}Ar-^{39}Ar ages. A Cretaceous intrusive dredged along the western Nayarit scarp (DANA47A) cooled below 310°-270 °C at ~19 Ma but the AFT age indicates a last exhumation at ~12 Ma. The AFT age of this sample is particularly interesting because the Nayarit scarps lies on the southeast margin of the Tamayo trough, which is interpreted by Sutherland et al. (2012) as highly stretched continental crust. Using gravity and magnetic data and layer thickness constrained by the seismic profile of Sutherland et al. (2012), Abera et al. (2016) reinterpret the Tamayo trough as a truly oceanic crust that separated the western Mexico margin from the Tamayo block, which in turn is a continental fragment separating the Tamayo trough from the Alarcón basin to the NW (Figs. 1 and 2). Abera et al. (2016) suggest that the Tamayo trough oceanic crust formed by the northern propagation of the Maria Magdalena Rise, a short-lived oceanic ridge located immediately to the south formed in the early Pliocene (Lonsdale, 1989). Our new ages suggest that extension leading to the formation of the Tamayo trough is middle to late Miocene, which also agree with the ~11 Ma old age of faulting in the basin suggested by Sutherland et al. (2012; their Table 1). The Cretaceous monzogranite of Sayulita (SAYU02), is exposed along the coast of Mexican mainland in Nayarit, along the NE-trending faults bounding the Jalisco Block at the mouth of the Gulf of California (Figs. 1 and 2). The sample yielded an Eocene biotite age and AFT age of ~10 Ma (Fig. 6). Even if the abanico curve suggests two age components (Fig. 3), the sample passes the χ^2-test and shows a dispersion below 20%, thus we do not deconvolve it.

The Early Miocene monzogranite ORO01, emplaced on the western border of the Sierra Madre Occidental in the footwall of the NNW-trending Pochititán fault system (Ferrari et al., 2013; Duque-Trujillo et al., 2014), shows a rapid cooling to the ^{40}Ar-^{39}Ar K-feldspar closure temperature at 17.6 Ma but, an AFT age of ~10 Ma (Fig. 6). In these three samples the Miocene AFT ages may represent a last phase of exhumation, also supported by the widespread occurrence of mafic dikes and lava flows dated at about 10–11 Ma both along the Nayarit coast and offshore (Ferrari et al., 2013; Duque-Trujillo et al., 2014).

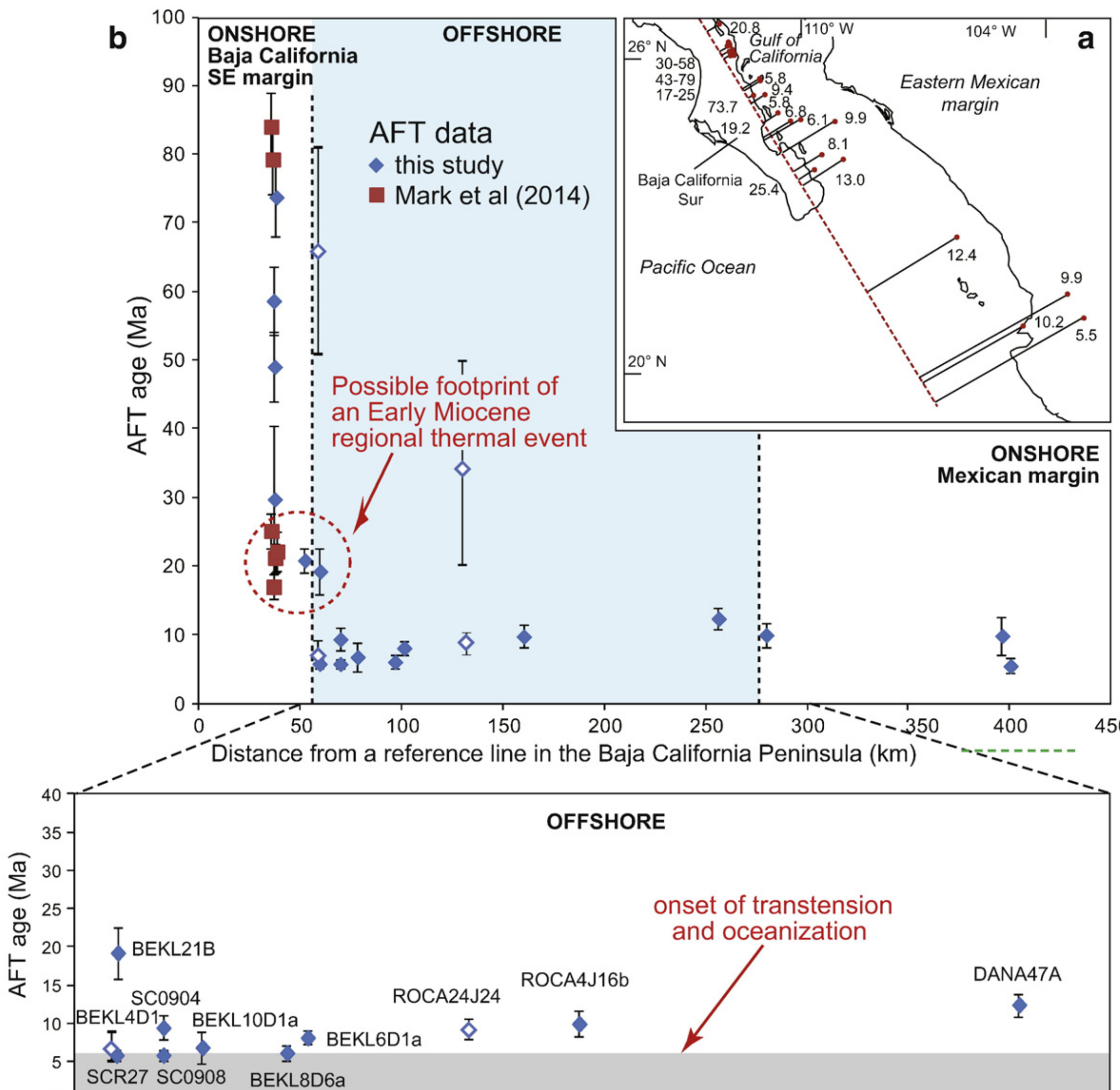

Fig. 8. AFT data projected onto a transect orthogonal to a reference line that approximates the crest of the rift escarpment in the Baja California Sur Peninsula. (a) Sketch map of Gulf of California region with AFT ages; the reference line and sample distances from the reference line are also shown. (b) AFT ages with 1s error bars are plotted according to the distance in kilometers from the reference line. Open diamonds are the minimum ages after deconvolution of the single grain age distributions.

4.4. Faulting in the Tepic-Zacoalco rift

The last sample is an Early Miocene Tonalite (BARR04) from the base of the WNW-ENE striking Plan de Barrancas normal fault (Fig. 2), which is part of the Tepic-Zacoalco rift. Ferrari (1995) proposed that the Tepic-Zacoalco rift is superimposed on a Middle to Late Miocene shear zone at the boundary between the Sierra Madre Occidental and the Jalisco Block. Based on geologic relations Ferrari and Rosas-Elguera (2000) estimated that the normal motion along the Plan de Barrancas fault mostly occurred in the early Pliocene. The BARR04 sample has an intrusion age of 22.6 Ma and overlapping ^{40}Ar-^{39}Ar hornblende and biotite ages of ca. 19 Ma, which point to a rapid cooling in the early Miocene (Fig. 6). The last exhumation is in latest Miocene (AFT age of 5.5 $\pm$ 1.1 Ma), which is consistent with the activity of this part of the Tepic-Zacoalco rift as determined by geologic data (Ferrari and Rosas-Elguera, 2000).

5. An AFT transect across the Gulf of California: hints into the time space evolution of the rifting

To facilitate a general discussion on the meaning of the AFT ages, we have plotted the AFT data along an ideal transect across the Gulf of California, from the eastern margin of Baja California Sur up to the Mexico mainland, in Nayarit (Fig. 8). Given the uncertainties on the kinematics and evolution of deformation within the Gulf, we have plotted the datapoints according to their distance from a reference line that approximates the crest of the rift escarpment in the Baja California Sur Peninsula (Fig. 8). We note that in the western domain, the AFT data are relatively old and range from ca. 70 Ma to 17 Ma, but immediately to the east they suddenly drop to younger values that group approximately around 6 Ma (Fig. 8). Further east, on the sheared margins of the Pescadero basin and in the eastern rifted margin offshore and onshore the trend of the AFT ages grow again up to ~10–12 Ma (Fig. 1).

We interpret the Early Miocene AFT ages (Mark et al., 2014; this study) as a possible footprint of a regional thermal event at ca. 25–20 Ma, which is mostly recorded along the eastern margin of the Baja California block (Fig. 8). This event might be related with the onset of early extension, which is now well documented in mainland Mexico, and that has been proposed to have affected a wide sector extending from eastern Baja California to the Sierra Madre Occidental (Ferrari et al., 2013, 2016; Bryan et al., 2014; Duque-Trujillo et al., 2015) (Fig. 9). This interpretation also finds support in the recently-proposed Early-Middle Miocene activity of the Los Barriles detachment, on the northern prolongation of the San José del Cabo detachment fault (Bot et al., 2016).

The AFT ages on both sides of the Pescadero basin indicate that intrusive rocks along the bounding strike-slip faults were being exhumed to very shallow level at 11–10 Ma, which suggest that this pull-apart oceanic basin evolved from a transtensional basin formed soon after the end of subduction, as suggested by Fletcher et al. (2007). Similar ages are reported for the initiation of the Gulf of California Shear Zone, a corridor of dextral transtensional deformation that started localizing the plate boundary in the northern Gulf between 12.4 and 6.5 Ma cutting across the wide rift zone of the Basin and Range province (Bennett and Oskin, 2014). However, in the northern Gulf this transtensional shear zone has been abandoned and the current plate boundary is located to the west, in the Delfin, Wagner and Consag pull-apart basins (Aragón-Arreola and Martín-Barajas, 2007; Martín-Barajas et al., 2013). In the southern Gulf, although the present plate boundary is still in the Pescadero and Farallón basin, it is remarkable that the youngest AFT ages (~6 Ma) are localized in a NNW-SSE-trending belt to the west of these basins (Figs. 8 and 9). This may be explained if this belt west of the Pescadero and Farallon basins is starting to accommodate part of the regional plate transtension since the end of Late Miocene and that this deformation is localizing along a rheological boundary of the relatively strong Baja California continental block. Evidence of this deformation event can be also found onshore (Umhoefer, 2011). In particular, Mark et al. (2014) inferred through AHe dating that crustal extension at Loreto began between ca. 8 and 6 Ma (Fig. 10). Despite the strong obliquity of the plate boundary, the deformation in this zone is seemingly characterized by extension. In particular, an array of N-S-to-NNW-trending Quaternary, active normal faults have been documented along the eastern margin of the Los Cabos Block in southern Baja California (e.g. San Juan de Los Planes faults, Coyan et al., 2013; El Carrizal fault, Umhoefer et al., 2014; San José del Cabo fault, Fletcher and Munguía, 2000; Fletcher et al., 2000) (Figs. 2 and 10). Focal mechanism solutions of earthquakes also indicate a consistent, dominant extensional fault kinematics in this area (Fletcher and Munguía, 2000;

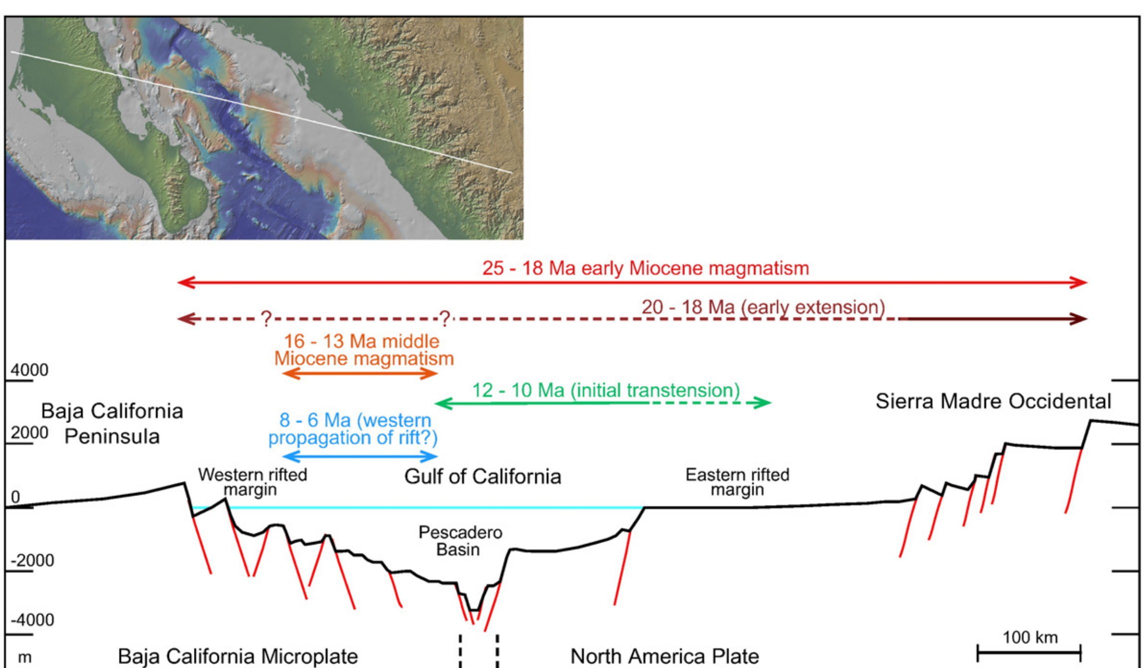

Fig. 9. Schematic profile showing the different domains of plutonism and extension deduced by combining ^{40}Ar-^{39}Ar and AFT cooling ages (colored arrows with ages). The trace of the profile is shown in digital elevation model of the upper panel.

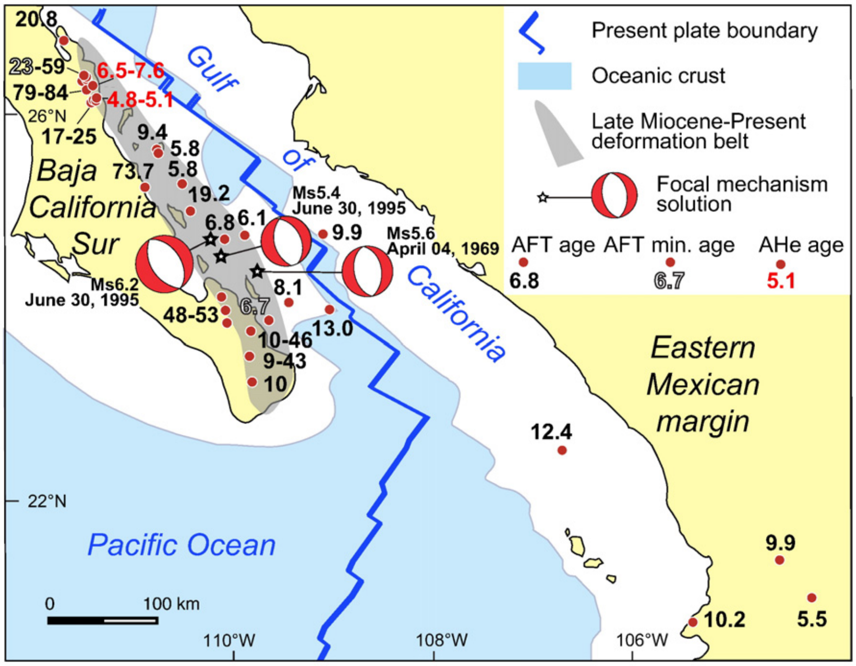

Fig. 10. Sketch map showing the main deformation features and AFT and AHe data in the southern Gulf of California. The data highlight the presence of a NNW-SSE-trending extensional deformation belt (gray shading) running along the eastern boundary of the Baja California block, and active from the Late Miocene to the Present. AFT ages are from this study, as well as from the literature (Fletcher et al., 2000; Mark et al., 2014). AHe ages are from Mark et al. (2014). The focal mechanism solutions of earthquakes are from Fletcher and Munguía (2000).

Umhoefer et al., 2014) (Fig. 10). Our data suggest that the NNW-SSE-trending extensional deformation belt along the eastern boundary of the Baja California block, would have been active since the end of Late Miocene to the Present.

6. Concluding remarks

The new AFT datasets on subaerial and submerged samples collected from the Gulf of California area have allowed to better constrain the time-space evolution of the rifting along a transect extending from Baja California peninsula to mainland Mexico. In particular, the availability of submerged samples already dated with high-temperature chronological methods (U-Pb zircon and ^{40}Ar-^{39}Ar hornblende, biotite and feldspar) has allowed us, for the first time, to make inferences on the timing of fault activity in this poorly accessible area. In particular, the results of the AFT analysis led to the following main conclusions:

1. An early Miocene thermal event is suggested in the eastern Baja California Peninsula. This event may be related to the localization of volcanism in this part of the Peninsula, but we cannot rule out that the early extension that has been proposed within the Gulf of California by Duque-Trujillo et al. (2015) and well documented in the eastern gulf margin in the states of Sinaloa and Nayarit (Ferrari et al., 2013) might have reached the easternmost Baja California. This last proposition requires further geological evidences along the Baja California eastern margin.
2. Intrusive rocks on the sheared margins of the Pescadero basin show 9–10 Ma AFT ages, which suggest that transtension was ongoing in this part of the Gulf soon after the end of subduction. The rifted margin to the east (both offshore and onshore) displays the same 12–10 Ma AFT ages. This age marks the latest pulse of tectonic activity for this area, concurrent with widespread mafic volcanism and the possible formation of the abandoned oceanic basin in the Tamayo trough.
3. The youngest AFT ages are located along a relatively narrow belt running in a ~NNW direction along the eastern boundary of the Baja California block, between the present plate boundary and the Baja California islands. Such an age distribution suggests that, since the end of Late Miocene (8–6 Ma), part of the extensional deformation is being accommodated to the west of the Pescadero and Farallón basins along the rheological boundary of the Baja California continental block.
4. A latest Miocene AFT age (5.5 Ma) for the Plan de Barrancas fault confirms that normal faulting in the Tepic–Zacoalco rift post-dated extensional faulting associated with the Gulf of California rift.

Acknowledgments

We would like to thank Chris Mark and an anonymous reviewer for their careful review and the useful suggestions that greatly improved the quality of this paper. This research has been funded by grant CONACYT 82378 (to Luca Ferrari) and the Postgraduate Program in Earth Science of UNAM. Progetto di Mobilità dei Ricercatori "Analisi della dinamica di apertura del Golfo della California" (Responsabile italiano Giacomo Corti, Responsabile messicano Mariano Cerca) inserito nel Programma Esecutivo del Ministero Affari esteri Italia – Messico 2011–2013.

References

Abera, R., Van Wijk, J., Axen, G., 2016. Formation of continental fragments: the Tamayo Bank, Gulf of California, Mexico. Geology 44 (8):595–598. http://dx.doi.org/10.1130/G38123.1.

Alexandre, P., 2011. Comparison between grain size and multi-mineral 40Ar/39Ar thermochronology. Geochim. Cosmochim. Acta 75 (15), 4260–4272.

Aragón-Arreola, M., Martín-Barajas, A., 2007. Westward migration of extension in the northern Gulf of California, Mexico. Geology 35 (6):571. http://dx.doi.org/10.1130/G23360A.1.

Barbarand, J., Carter, A., Wood, I., Hurford, T., 2003. Compositional and structural control of fission-track annealing in apatite. Chem. Geol. 198, 107–137.

Bennett, S.E.K., Oskin, M.E., 2014. Oblique rifting ruptures continents: example from the Gulf of California shear zone. Geology 42 (3):215–218. http://dx.doi.org/10.1130/G34904.1.

Bennett, S.E.K., Oskin, M.E., Iriondo, A., 2013. Transtensional rifting in the proto-Gulf of California near Bahia Kino, Sonora, Mexico. Geol. Soc. Am. Bull. 125 (11–12): 1752–1782. http://dx.doi.org/10.1130/B30676.1.

Bhandari, N., Bhat, S.C., Lal, D., Rajagoplan, G., Tamhane, A.S., Venka-Tavaradan, V.S., 1971. Fission fragment tracks in apatite: recordable track lengths. Earth Planet. Sci. Lett. 13, 191–199.

Bot, A., Geoffroy, L., Authemayou, C., Bellon, H., David, G., Raphaël, P., 2016. Miocene detachment faulting predating EPR propagation: Southern Baja California. Tectonics: 1–24 http://dx.doi.org/10.1002/(ISSN)1944-9194.

Brandon, M.T., Roden-Tice, M.K., Garver, J., 1998. Late Cenozoic exhumation of the Cascadia accretionary wedge in the Olympic Mountains, northwest Washington State. Geol. Soc. Am. Bull. 110:985–1009. http://dx.doi.org/10.1130/0016-7606(1998)110.

Bryan, S.E., Orozco-Esquivel, T., Ferrari, L., López-Martínez, M., 2014. Pulling apart the Mid to Late Cenozoic magmatic record of the Gulf of California: is there a Comondú arc? In: Gómez-Tuena, A., Straub, S.M., Zellmer, G.F. (Eds.), Orogenic Andesites and Crustal Growth. 385. Geological Society of London, Special Publication:pp. 389–407. http://dx.doi.org/10.1144/SP385.8

Cherniak, D.J., Watson, E.B., 2001. Pb diffusion in zircon. Chem. Geol. 172:5–24. http://dx.doi.org/10.1016/S0009-2541(00)00233-3.

Coyan, M.M., Arrowsmith, J.R., Umhoefer, P., Coyan, J., Kent, G., Driscoll, N., Martínez-Gutiérrez, G., 2013. Geometry and quaternary slip behavior of the San Juan de los Planes and Saltito fault zones, Baja California Sur, Mexico: characterization of rift-margin normal faults. Geosphere http://dx.doi.org/10.1130/GES00806.1.

Dixon, T., Farina, F., DeMets, C., et al., 2000. New kinematic models for Pacific-North America motion from 3 Ma to present, II: evidence for a "Baja California Shear Zone". Geophys. Res. Lett. 27 (23):3961–3964. http://dx.doi.org/10.1029/2000GL008529.

Dunkl, I., 2002. TRACKKEY: a Windows program for calculation and graphical presentation of fission track data. Comput. Geosci. 28:3–12. http://dx.doi.org/10.1016/S0098-3004(01)00024-3.

Duque-Trujillo, J., Ferrari, L., Norini, G., Lopez-Martinez, M., 2014. Miocene faulting in the southwestern Sierra Madre Occidental, Nayarit, Mexico: kinematics and segmentation during the initial rifting of the southern Gulf of California. Rev. Mex. Cienc. Geol. 31 (3):283–302. http://dx.doi.org/10.2307/41170048.

Duque-Trujillo, J., Ferrari, L., Orozco-Esquivel, T., López-Martínez, M., Lonsdale, P., Bryan, S.E., Kluesner, J., Piñero-Lajas, D., Solari, L., 2015. Timing of rifting in the southern Gulf of California and its conjugate margins: insights from the plutonic record. GSA Bull. 127:702–736. http://dx.doi.org/10.1130/B31008.1.

Ferrari, L., 1995. Miocene shearing along the northern boundary of the Jalisco block and the opening of the southern Gulf of California. Geology 23:751–754. http://dx.doi.org/10.1130/0091-7613(1995)023<0751.

Ferrari, L., Rosas-Elguera, J., 2000. Late Miocene to Quaternary extension at the northern boundary of the Jalisco block, western Mexico: the Tepic-Zacoalco rift revised. Geol. Soc. Am. Spec. Pap.:42–64 (#334, chapter 03). 10.1016/S0040-1951(99)00310-8.

Ferrari, L., Orozco-Esquivel, T., Manea, V., Manea, M., 2012. The dynamic history of the Trans-Mexican Volcanic Belt and the Mexico subduction zone. Tectonophysics 522–523:122–149. http://dx.doi.org/10.1016/j.tecto.2011.09.018.

Ferrari, L., López-Martínez, M., Orozco-Esquivel, T., Bryan, S.E., Duque-Trujillo, J., Lonsdale, P., Solari, L., 2013. Late Oligocene to middle Miocene rifting and syn-extensional magmatism in the southwestern Sierra Madre Occidental, Mexico: the beginning of the Gulf of California rift. Geosphere 9:1161–1200. http://dx.doi.org/10.1130/GES00925.1.

Ferrari, L., Orozco, Esquivel T., Bryan, S.E., López, Martínez M., Silva Fragoso, A., 2016. Cenozoic Extension and Magmatism in Western Mexico: Linking the Sierra Madre Occidental Silicic Large Igneous Province and the Comondú Group With the Gulf of California Rift. (Submitted to Earth Science Review, May). .

Fletcher, J.M., Munguía, L., 2000. Active continental rifting in southern Baja California, Mexico: implications for plate motion partitioning and the transition to seafloor spreading in the Gulf of California. Tectonics 19:1107–1123. http://dx.doi.org/10.1029/1999TC001131.

Fletcher, J.M., Kohn, B.P., Foster, D.A., Gleadow, A.J.W., 2000. Heterogeneous Neogene cooling and exhumation of the Los Cabos block, southern Baja California: evidence from fission-track thermochronology. Geology 28:107–110. http://dx.doi.org/10.1130/0091-7613(2000)28<107:HNCAEO>2.0CO;2.

Fletcher, J.M., Grove, M., Kimbrough, D., Lovera, O., Gehrels, G.E., 2007. Ridge-trench interactions and the Neogene tectonic evolution of the Magdalena shelf and southern Gulf of California: insights from detrital zircon U-Pb ages from the Magdalena fan and adjacent areas. Geol. Soc. Am. Bull. 119:1313–1336. http://dx.doi.org/10.1130/B26067.1.

Galbraith, R.F., 1981. On statistical models of fission track count. Math. Geol. 13:471–488. http://dx.doi.org/10.1007/BF01033028.

Galbraith, R.F., 1988. Graphical display of estimates having differing standard errors. Tectonometrics 30, 271–281.

Galbraith, R.F., Green, P.F., 1990. Estimating the component ages in a finite mixture. International Journal of Radiation Applications and Instrumentation. Part D. Nuclear Tracks and Radiation Measurements 17 (3), 197–206.

Galbraith, R.F., Laslett, G.M., 1993. Statistical models for mixed fission track ages. Nuclear tracks and radiation measurements 21 (4), 459–470.

Gallagher, K., 1995. Evolving temperature histories from apatite fission-track data. Earth Planet. Sci. Lett. 136, 421–435.

Gans, P.B., 1997. Large-magnitude Oligo-Miocene extension in southern Sonora, implications for the tectonic evolution of northwest Mexico. Tectonics 16:388–408. http://dx.doi.org/10.1029/97TC00496.

Godinez, N.S., Kimbrough, D.L., Kohel, C., 2010. Stratigraphy and petrologic evolution of the Oligocene–Miocene Comondú Group near Bahia Concepcion and Loreto, Baja California Sur, Mexico. Geol. Soc. Am. Abstr. Programs 42 (4), 66.

Green, P.F., Duddy, I.R., 1989. Some comments on paleotemperature estimation from apatite fission tracks analysis. J. Pet. Geol. 12:111–114. http://dx.doi.org/10.1111/j.1747-5457.1989.tb00224.x.

Hausback, B.P., 1984. Cenozoic volcanism and tectonic evolution of Baja California Sur, Mexico. In: Frizzell Jr., V.A. (Ed.), Geology of the Baja California Peninsula. 39. Pacific Section Society of Economic Paleontologists and Mineralogists, pp. 219–236.

Hurford, A.J., 1990. Standardization of fission track dating calibration: recommendation by the Fission Track Working Group of the I.U.G.S.Sub commission on geochronology. Chem. Geol. 80, 171–178.

Ketcham, R.A., 2005. Forward and inverse modeling of low-temperature thermochronometry data. Rev. Mineral. Geochem. 58:275–314. http://dx.doi.org/10.2138/rmg.2005.58.11.

Ketcham, R.A., Donelick, R.A., Donelick, M.B., 2000. AFTSolve: a program for multi-kinetic modeling of apatite fission-track data. Geol. Mater. Res. 2, 1–32.

Lonsdale, P., 1989. Geology and tectonic history of the Gulf of California. In: Hussong, D., Winterer, E.L., Decker, R.W. (Eds.), The Eastern Pacific Ocean and Hawaii. Vol. N of The Geology of North America. Geological Society of America Boulder, CO, pp. 499–522.

Lonsdale, P., 1991. Structural Patterns of the Pacific Floor Offshore of Peninsular California. AAPG Memoir, M 47: The Gulf and Peninsular Province of the California, Chapter 7: Part III. Regional Geophysics and Geology. pp. 87–110.

Mark, C., Gupta, S., Carter, A., Mark, D.F., Gautheron, C., Martín, A., 2014. Rift flank uplift at the Gulf of California: no requirement for asthenospheric upwelling. Geology 42 (3): 259–262. http://dx.doi.org/10.1130/G35073.1.

Martín-Barajas, A., González-Escobar, M., Fletcher, J.M., Pacheco, M., Oskin, M., Dorsey, R., 2013. Thick deltaic sedimentation and detachment faulting delay the onset of continental rupture in the Northern Gulf of California: Analysis of seismic reflection profiles. Tectonics 32 (5), 1294–1311.

McDowell, F., Roldán-Quintana, J., Amaya-Martínez, R., 1997. Interrelationship of sedimentary and volcanic deposits associated with tertiary extension in Sonora, Mexico. Geol. Soc. Am. Bull. 109:1349–1360. http://dx.doi.org/10.1130/00167606(1997)109<1349:IOSAVD>2.3.CO;2.

McFall, C.C., 1968. Reconnaissance Geology of the Concepcion Bay Area, Baja California, Mexico. Vol. 10, No. 5. School of Earth Sciences. Stanford University.

Ortega-Gutierrez, F., Elías-Herrera, M., Moran-Zenteno, D.J., Solari, L., Luna-González, L., Schaaf, P., 2014. A review of batholiths and other plutonic intrusions of Mexico. Gondwana Res. 26 (3–4):834–868. http://dx.doi.org/10.1016/j.gr.2014.05.002.

Oskin, M., Stock, J., Martin-Barajas, A., 2001. Rapid localization of Pacific-North America plate motion in the Gulf of California. Geology 29:459–462. http://dx.doi.org/10.1130/0091-7613(2001)029<0459:RLOPNA>2.0.CO;2.

O'Sullivan, P.B., Parrish, R.R., 1995. The importance of apatite composition and single-grain ages when interpreting fission track data from plutonic rocks: a case study from the Coast Ranges, British Columbia. Earth Planet. Sci. Lett. 132, 213–224.

Plattner, C., Malservisi, R., Dixon, T.H., LaFemina, P., Sella, G.F., Fletcher, J., Suarez-Vidal, F., 2007. New constraints on relative motion between the Pacific Plate and Baja California microplate (Mexico) from GPS measurements. Geophys. J. Int. 170:1373–1380. http://dx.doi.org/10.1111/j.1365-246X.2007.03494.x.

Reiners, P.W., Ehlers, T.A., Zeitler, P.K., 2005. Past, present, and future of thermochronology. Rev. Mineral. Geochem. 58:1–18. http://dx.doi.org/10.2138/rmg.2005.58.1.

Seiler, C., Fletcher, J.M., Quigley, M.C., Gleadow, A.J.W., Kohn, B.P., 2010. Neogene structural evolution of the Sierra San Felipe, Baja California: evidence for proto-gulf transtension in the Gulf Extensional Province? Tectonophysics 488:87–109. http://dx.doi.org/10.1016/j.tecto.2009.09.026.

Stock, J.M., Hodges, K.V., 1989. Pre-Pliocene extension around the Gulf of California and the transfer of Baja California to the Pacific plate. Tectonics 8, 99–115.

Stock, J., Lee, J., 1994. Do microplates in subduction zones leave a geological record. Tectonics 13 (6), 1472–1487.

Sutherland, F.H., Kent, G.M., Harding, A.J., Umhoefer, P.J., Driscoll, N.W., Lizarralde, D., Fletcher, J.M., Axen, G.J., Holbrook, W.S., González-Fernández, A., Lonsdale, P., 2012. Middle Miocene to early Pliocene oblique extension in the southern Gulf of California. Geosphere 8:752–770. http://dx.doi.org/10.1130/GES00770.1 (2012).

Umhoefer, P.J., 2011. Why did the Southern Gulf of California rupture so rapidly?—oblique divergence across hot, weak lithosphere along a tectonically active margin. GSA Today 21 (11):4–10. http://dx.doi.org/10.1130/G133A.1.

Umhoefer, P.J., Maloney, S.J., Buchanan, B., Arrowsmith, J.R., Martinez-Gutiérrez, G., Kent, G., Driscoll, N., Harding, A., Kaufman, D., Rittenour, T., 2014. Late Quaternary faulting history of the Carrizal and related faults, La Paz region, Baja California Sur, Mexico. Geosphere 10, 476–504 (doi:10.1130/GES00924.1. doi: 10.1130/G133A.1).

Vermeesch, P., 2009. RadialPlotter: a Java application for fission track, luminescence and other radial plots. Radiat. Meas. 44 (4):409–410. http://dx.doi.org/10.1016/j.radmeas.2009.05.003.

Wagner, G.A., Van de Haute, P., 1992. Fission-track Dating. vol. 6. Springer Science & Business Media, pp. 1–285.

Wong, M.S., Gans, P.B., Scheier, J., 2010. The 40Ar/39Ar thermochronology of core complexes and other basement rocks in Sonora. Mexico: Implications for Cenozoic tectonic evolution of northwestern Mexico. Journal of Geophysical Research: Solid Earth 115 (B07414):pp. 19. http://dx.doi.org/10.1029/2009JB007032.